

Article

Three-Dimensional Obstacle Avoidance Path Planning for Agricultural UAV Based on Improved Ant Colony Algorithm

Yi Shao¹, Hua Yang², Ruibo Gao², and Fuzhong Li^{3,*}¹ College of Agricultural Engineering, Shanxi Agricultural University, Taigu, Shanxi, China² College of Information Science and Engineering, Shanxi Agricultural University, Taigu, Shanxi, China³ School of Software, Shanxi Agricultural University, Taigu, Shanxi, China

* Correspondence: lifuzhong@sxau.edu.cn

Received: 30 May 2025

Accepted: 10 October 2025

Published: 18 December 2025

Abstract: Obstacle avoidance is crucial for unmanned aerial vehicles (UAVs) in agriculture to perform tasks such as crop monitoring, precision spraying and picking assistance. The three-dimensional (3D) nature of orchards, with issues such as a larger search space, diverse obstacle shapes, and higher requirements for environmental adaptability, poses challenges for UAV obstacle avoidance. In this paper, a 3D obstacle avoidance path planning method for agricultural UAVs based on improved ant colony optimization (ACO) algorithm is proposed. Firstly, A 3D orchard simulation environment is constructed using MATLAB. Secondly, based on the characteristics of the orchard environment with large ups and downs of the terrain and multiple obstacles, the fitness function and heuristic information in the ACO algorithm have been modified. Thirdly, a leader ant optimization (LAO) algorithm is proposed by introducing the bellwether theory to improve the ACO algorithm. The LAO algorithm has been comprehensively evaluated on path optimal solution, obstacle avoidance capability, convergence speed and computation time. The experimental results demonstrate that the performance of LAO algorithm is optimal compared to the traditional ACO algorithm, genetic algorithm (GA) and particle swarm optimization (PSO) algorithm. The proposed LAO algorithm is suitable for UAV obstacle avoidance in orchards.

Keywords: improved ACO algorithm; agricultural UAV; 3D path planning; obstacle avoidance

1. Introduction

Agriculture unmanned aerial vehicles (UAVs) are often used for tasks such as orchard monitoring, pesticide spraying and data collection [1–4]. Agricultural UAVs often encounter problems of multiple obstacles, uneven terrain, precision operations, and dynamic environment when flying in complex orchard environments [5–7]. Commonly used two-dimensional (2D) path planning methods are difficult to meet the needs of practical applications. To solve these problems, the three-dimensional (3D) obstacle avoidance path planning method for agricultural UAVs is necessary.

In the study of path planning, 2D methods and 3D methods exhibit fundamental differences in terms of environmental modeling and search space dimensionality. The 2D methods are mostly based on discretized planar grids, where obstacles in the environment are projected onto a 2D plane for processing. This approach has low computational cost and is suitable for fast in-contour planning on flat terrain. In contrast, by introducing the height information, 3D planning provides 3D routes that aligns with actual flight and safety requirements. On the other hand, the size of the state space to be processed increases exponentially, and the amount of computation and storage for neighborhood search and collision detection increase significantly. The existing 3D path planning algorithms mainly include the A* algorithm, genetic algorithm (GA), particle swarm optimization (PSO) algorithm [8–10]. However, the computational complexity of the A* algorithm increases dramatically when it is extended to a 3D environment,



while the GA and PSO algorithms also suffer from the shortcomings such as poor adaptability to dynamic environments and the easy to fall into local optimal solutions. Therefore, the problems of planning paths in 3D space with computational complexity, dynamic environment adaptability, multi-objective optimization and global optimality remain to be solved [11–13].

In search of an algorithmic candidate for 3D route planning for agricultural UAVs, the ant colony optimization (ACO) algorithm has been proposed due to its natural adaptation to path optimization problems with strong dynamic adaptability and global search capability [14,15]. However, the direct application of traditional ACO algorithms in 3D path planning still suffers from some problems, such as slow convergence, easy to fall into local optimum or unsafe paths [16–19]. To address these issues, researchers have proposed a series of improvements [20,21]. For example, in environment modeling, continuous picking path planning is abstracted as a 3D traveling salesman problem (TSP) by Zhang et al. [22], which achieves continuous path optimization while ignoring obstacles. In terms of heuristic information optimization, the safety value function is proposed by Wang et al. [23] and incorporated into the heuristic function of the ACO algorithm, improving the efficiency of path planning and enabling effective obstacle avoidance. With respect to the improvement of the pheromone mechanism, the pheromone update strategy is improved by Duan et al. [24] using a differential evolutionary algorithm, accelerating the global convergence of the algorithm. The pheromone structure of traditional ACO is extended from 2D to 3D by Guo et al. [25], significantly improving the accuracy of solution reconstruction. The pheromone update mechanism is improved by Chen et al. [26] in terms of path factor, turn factor and security factor to solve the problem of deadlock and poor security. The environment is modeled with a 3D grid method, and the pheromone reset method is proposed by Pu et al. [27] to maintain the diversity of solutions and avoid deadlocks. Regarding the search strategy, the search dimension of the ACO algorithm is further extended by Zhang et al. [28], and a 3D ACO algorithm is proposed to expand the selection of nodes to the 3D space of “longitude-latitude-velocity”. In multi-objective optimization, with safe obstacle avoidance and shortest path as the optimization objectives, new heuristic factors, node selection optimization and pheromone updating mechanisms are introduced by Li & Yu [29], showing good decision-making ability and convergence performance. The multi-objective function integrating path distance and corner is established by Zhou et al. [30], and a goal-guidance mechanism and an anti-deadlock mechanism are also designed to enhance the goal-directedness of the search process. Furthermore, in combination with other algorithms, localized pheromones in 3D space are adjusted by Han et al. [31] with the help of artificial potential field directional information, which enhances the directionality of the path towards the target point and speeds up the convergence of the algorithm. An improved ACO algorithm incorporating subpopulation mechanism based on adaptive heuristic factors and prior knowledge guidance strategy is proposed by Song et al. [32], which enhances the global search capability and accelerates the convergence speed. To solve the problem that the traditional ACO algorithm is prone to fall into local optimum, the beetle antennae search (BAS) algorithm is introduced by Yan et al. [33] to perform quadratic programming on the paths, thereby improving the speed and stability of the path search.

Although a number of works can help to improve the search capability and convergence speed of traditional ACO in 3D path optimization, there are still some challenges in the practical application to agricultural operations using UAVs. Among them, the obstacle avoidance problem has attracted widespread attention due to its critical role in ensuring UAV flight safety. For example, to deal with the flight safety problems caused by the unstructured layout of orchards and the irregular distribution of obstacles, an obstacle detection method based on the fusion of ultrasonic wave and monocular vision is proposed by Yu [34], which realizes autonomous obstacle avoidance of UAVs by detecting the information of obstacle edge contours. The deep Q-learning network is adopted by Tu & Juang [35] to enable UAVs to realize real-time visual obstacle avoidance in virtual environments by learning from deep images. Meanwhile, an ultrasonic sensor module is introduced to achieve stable sensing and avoidance of lateral obstacles. Recently, deep neural networks are introduced into the improved Q-learning algorithm by Zhang et al. [36], enhancing the capability of the algorithm for dynamic obstacle detection and real-time avoidance in complex 3D orchard environments. The depth map back-projection algorithm is used by Liu et al. [37] to compute the 3D point cloud of obstacles in the global coordinate system, effectively solving the redundancy and complexity problems in the construction of orchard maps.

In addition, there are other challenges for UAVs to avoid obstacles in the orchard environment. Firstly, the structure of the orchard environment is complex. Fruit trees are densely distributed, and the canopy and trunks are prone to visual occlusion, making obstacle perception difficult. Secondly, dynamic obstacles exist. There are often staff, agricultural machinery and other dynamic obstacles in the orchard operation process, which puts forward higher requirements for real-time obstacle avoidance and path planning. Thirdly, computational resources are limited. The limited computational capacity of UAVs makes it difficult to realize real-time obstacle avoidance planning with high precision and rapid responsiveness.

In summary, the aim of this paper is to propose a 3D obstacle avoidance path planning method for agricultural UAVs based on the improved ACO algorithm. Combining the characteristics of the orchard environment, the fitness function and heuristic information in the ACO algorithm are changed. In addition, by introducing the bellwether theory to improve the ACO algorithm, a novel leader ant optimization (LAO) algorithm is proposed. Finally, the effectiveness of the method is verified by simulation experiments.

The main contributions of this paper are as follows:

1. According to the constructed virtual scene of a 3D orchard with large ups and downs of the terrain and multiple obstacles, the fitness function and heuristic information of the ACO are altered. It becomes possible to realize obstacle avoidance for agricultural UAVs using the ACO algorithm. 2. A new LAO algorithm is proposed by combining the bellwether theory and the ACO algorithm. The problem of slow convergence and easily falling into the local optima of ACO algorithm is solved. 3. Simulation experiments show that the LAO algorithm outperforms the traditional ACO, GA and PSO algorithms in terms of path optimal solution, obstacle avoidance capability, convergence speed and computation time.

2. Basic ACO algorithm

The ACO algorithm, first proposed by Marco Dorigo in 1992, is a heuristic optimization algorithm that simulates the foraging behavior of ants in nature [38]. The ACO algorithm is also a colony intelligence algorithm that draws on the mechanism by which ants gradually find optimal paths through pheromone interactions in their search for food [39,40].

When searching for a food source, ants release a pheromone on the paths they pass through and are able to sense the pheromone left behind by other ants. When choosing a path, ants usually prioritize the path with higher pheromone concentration with a higher probability. And release a certain amount of pheromone to enhance the pheromone concentration on that path, forming a positive feedback. At the same time, the pheromone concentration on the path will gradually evaporate over time to avoid the algorithm from falling into local optimality. The size of the pheromone concentration represents the distance of the path, the higher the pheromone concentration, the shorter the distance of the corresponding path. Finally, the ant is able to find a shortest path from the nest to the food source, which is the global optimal solution.

The state transfer rules, pheromone update rules and heuristic functions of the ACO algorithm are described as follows:

(1)State transfer rules:

At time t , the ant chooses a node at random, and then the ant moves from node to node until it passes through all the nodes. Assuming that the current ant chooses to move to node j at node i , its selection probability can be expressed by the following equation:

$$P_{ij} = \frac{[\tau_{ij}]^\alpha [\eta_{ij}]^\beta}{\sum_{u \in N(i)} [\tau_{iu}]^\alpha [\eta_{iu}]^\beta} \quad (1)$$

where P_{ij} is the selection probability of the ant from node i to node j . τ_{ij} represents the pheromone concentration on the path between nodes i and j . η_{ij} is the value of the heuristic function for the path between nodes i and j . α and β indicate the importance factors of the pheromone and heuristic functions, respectively. $N(i)$ is the set of neighboring nodes of node i .

(2)Pheromone update rule:

Pheromone updating is a crucial step in the ACO algorithm that determines the ants' preferences on the path. Pheromone updating includes two parts: global pheromone updating and local pheromone updating.

Global updating refers to the global updating of the pheromone based on the quality of the path after the ants have completed the path planning. Path quality is usually evaluated based on the objective function values (e.g., total distance, total cost, etc.). The global pheromone update formula is:

$$\tau_{ij}(t+1) = (1-\rho) \cdot \tau_{ij}(t) + \sum_{k=1}^m \Delta\tau_{ij}^{(k)} \quad (2)$$

$$\Delta\tau_{ij}^{(k)} = \frac{Q}{L_k} \quad (3)$$

where $\tau_{ij}(t)$ represents the pheromone concentration on the path between nodes i and j at time t . ρ is the pheromone volatilization factor, which takes a value between 0 and 1, and indicates the volatilization rate of the pheromone.

$\Delta\tau_{ij}^{(k)}$ is the pheromone increment of the k th ant on the path between nodes i and j . m means the total number of ants. Q is a constant, usually proportional to the problem size or the number of ants. L_k denotes the length of the path found by the k th ant.

Local updating refers to the real-time updating of the pheromone concentration on a path as the ant selects the path. In general, the pheromone concentration will gradually decrease as the ants pass by during the path selection process. The formula for local update is as follows:

$$\tau'_{ij}(t+1) = (1 - \rho) \cdot \tau'_{ij}(t) + \rho \cdot \tau_0 \tag{4}$$

where $\tau'_{ij}(t)$ represents the pheromone concentration on the path between nodes i and j at time t . τ_0 is the initial concentration of pheromone in the path, usually a constant.

(3) Heuristic function:

In the ACO algorithm, the heuristic function is a tool that helps the ants to make decisions in path selection, and it is closely related to the nature of the actual problem. In path planning problem, to minimize the path length, the heuristic function is the reciprocal of the distance between nodes:

$$\eta_{ij} = \frac{1}{d_{ij}} \tag{5}$$

where d_{ij} indicates the distance from node i to node j .

3. A novel LAO algorithm

The ACO algorithm essentially models the behavior of ants in finding food paths, while the bellwether theory focuses on the role and function of the leader in the colony. A LAO algorithm is proposed which combines the bellwether theory with the ACO algorithm. The algorithm can improve the path selection and optimization process of the ACO algorithm by simulating the decision-making process of the leader role in the colony. To enhance understanding of the modifications introduced in LAO, the algorithm's workflow is depicted in [Figure 1](#). The details are as follows:

(1) Guided path selection:

By introducing the concept of "Leader Ant", which can lead other ants to a better direction according to the global information (e.g., the quality of the current path), and other ants imitate the behavior of the leader ant and gradually approach the optimal solution. The path selection probability formula for the LAO algorithm is as follows:

$$P_{ij}^l = \begin{cases} \frac{[\tau_{ij}]^\alpha [\eta_{ij}]^\beta}{\sum_{u \in N(i)} [\tau_{iu}]^\alpha [\eta_{iu}]^\beta}, & \text{If } l \text{ is a common ant} \\ \frac{[\tau_{ij}]^{\alpha+\delta} [\eta_{ij}]^{\beta+\delta'}}{\sum_{u \in N(i)} [\tau_{iu}]^{\alpha+\delta} [\eta_{iu}]^{\beta+\delta'}}, & \text{If } l \text{ is a leader ant} \end{cases} \tag{6}$$

where δ and δ' are the weight coefficients of the pheromone and heuristic information added to the leader ant, respectively. It represents the guiding effect of the leader ant's decision on path selection.

(2) Dynamic adjustment of pheromone updating rules:

If certain ants show better path selection (similar to the behavior of the leader), then the pheromone concentration can be increased for the paths where these ants are located. In this way, other ants are more likely to follow the path of the lead ant, thus accelerating the convergence of the algorithm. The pheromone update formula for the LAO algorithm is as follows:

$$\tau_{ij}(t+1) = (1 - \rho) \cdot \tau_{ij}(t) + \sum_l \Delta\tau_{ij}^l + \Delta\tau_{ij}^{lead} \tag{7}$$

$$\Delta\tau_{ij}^{lead} = \varphi_{lead} \cdot \Delta\tau_{ij}^l \tag{8}$$

where $\Delta\tau_{ij}^l$ is the pheromone contributed by the common ant l to the path between nodes i and j . $\Delta\tau_{ij}^{lead}$ is the pheromone of the additional contribution of the leader ant to the path between nodes i and j , which can be increased based on the quality of the path chosen by the leader ant or its leadership. φ_{lead} is a weight parameter indicating that the path contribution of the leader ant may be several times that of the common ant.

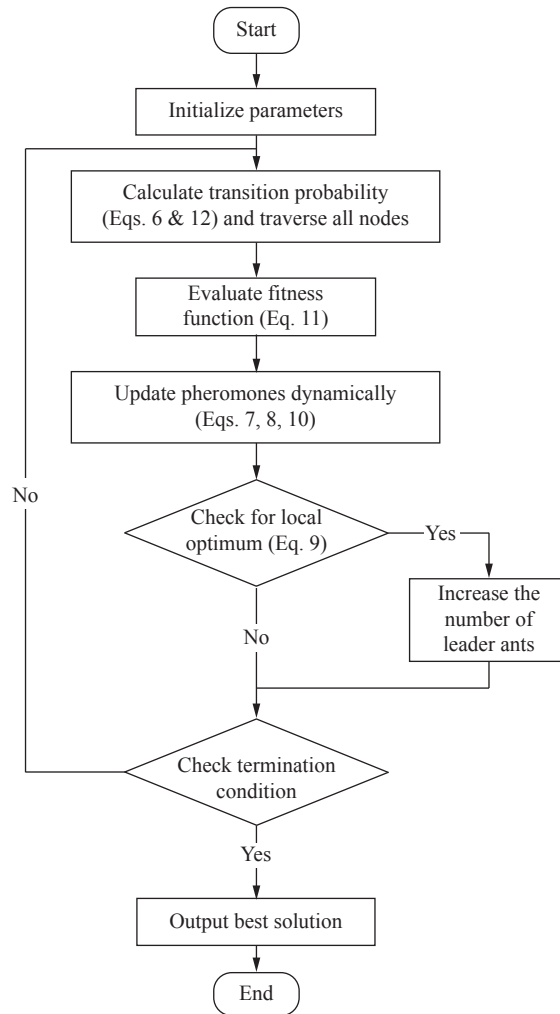


Figure 1. Flowchart of the proposed LAO algorithm.

(3) The ability to balance global and local search:

Adjusting the search strategy based on the behavior of the leader ants is used to enhance the global search capability. Specifically, in each round of iteration, the leader ants can lead some ants to explore farther regions to avoid the algorithm from falling into local optimal solutions. A dynamic threshold can be set to determine whether there is enough exploration space for the leader ants to lead other ants to jump out of the local optimal region. Adjusting the number of leader ants based on the current search state and global information, a dynamic adjustment mechanism is designed as follows:

$$\text{if } \frac{f(\text{current path})}{f(\text{global best})} < \varepsilon \text{ then increase the number of lead ants} \quad (9)$$

where $f(\text{current path})$ is the objective function value of the current path. $f(\text{global best})$ is the objective function value of the globally optimal path. ε is a certain predefined threshold.

(4) Collective decision making of the colony:

The leader ant in the LAO algorithm can have a large impact on the path selection of the whole colony. By introducing the guiding role of the leader ant, the weight allocation in collective decision-making is increased. At each update of the pheromone, a weight factor is added to specify the dominance of the path of the leader ant in the colony decision as follows:

$$\tau_{ij}(t+1) = (1-\rho) \cdot \tau_{ij}(t) + \sum_l \Delta\tau_{ij}^l + \omega_{lead} \cdot \Delta\tau_{ij}^{lead} \quad (10)$$

where ω_{lead} is the weight of the lead ant in the collective decision, which is usually greater than the contribution of the common ants.

(5) Calculate the adaptation value:

In order to adapt to the obstacle avoidance needs of UAVs in orchards, it is necessary to incorporate

consideration of obstacles, flight height, distribution of fruit trees, and other environmental factors in calculating the path adaptation. In an orchard, the “distance” of a path is not only the horizontal distance, but also the ups and downs of the terrain that need to be taken into account when the UAV is flying. The effect of height difference has a greater impact on path planning, especially if the UAV needs to cross higher fruit trees. The height data is used to determine whether the path collides with an obstacle or not. If the height of a point the path passes through exceeds the threshold, a collision is considered to have occurred and a penalty is added to the path. The fitness value is calculated as a weighted sum of distance, path height difference, and obstacle penalty as follows:

$$fitness = \mu_1 \cdot T_{distance} + \mu_2 \cdot T_{height} + \mu_3 \cdot C_{penalty} \quad (11)$$

where μ_1 , μ_2 , and μ_3 denote the weights of the path distance, path height difference and obstacle penalty, respectively. $T_{distance}$ represents the total length of the path. T_{height} indicates the total height of the path. $C_{penalty}$ means the collision penalty.

(6) Calculate the heuristic value:

The influence of orchard features is added to the calculation of the heuristic value, which makes the priority of path points in the obstacle and tree regions lower, thus avoiding these regions. According to the distribution of trees in the orchard or other obstacle information, the reachability judgment condition is modified. A point is considered unreachable if its height does not pass the height of the UAV or if it is covered by trees or shrubs. A height factor is introduced which is influenced by the height of fruit trees or different vegetation areas. It is assumed that if a point is in a tree area, the effect of the height factor increases, resulting in a smaller heuristic value, which avoids the UAV from flying over trees. The path distance is a combination of horizontal and vertical distances and height difference and is adjusted according to the shape of the path and obstacles. The heuristic value is the weighted sum of reachability, height factor and path distance as shown below:

$$\eta = \mu_4 \cdot S \cdot (\mu_5 \cdot M + \mu_6 \cdot D + \mu_7 \cdot P) \quad (12)$$

where μ_4 , μ_5 , μ_6 , and μ_7 indicate the weights of the reachability, height factor, distance factor, and smoothness factor, respectively. S means reachability. M represents the height factor. D denotes the distance factor. P is the smoothness factor.

4. Results and discussion

4.1. Experimental environment and parameter settings

The experimental platform is a PC with an 13th Gen Intel(R) Core(TM) i5-13400F @ 2.50 GHz CPU, 32.0 GB memory, NVIDIA GeForce RTX 4060 graphics, and Windows 11 operating system. And the experiments are performed in the software environment of MATLAB R2020a simulation platform.

The parameters used in the LAO algorithm are listed in Table 1. Among them, these parameters (m , T , α , β , and ρ) are configured according to commonly accepted empirical settings. In addition, the algorithm incorporates eight newly introduced parameters (L , μ_1 , μ_2 , μ_3 , μ_4 , μ_5 , μ_6 , and μ_7) to improve the effectiveness of path evaluation and guidance mechanisms. To ensure these parameters are optimally configured, a grid search combined with sensitivity analysis is conducted within reasonable parameter ranges. According to the specific demands of the 3D obstacle avoidance path planning task, a set of parameter values demonstrating favorable performance in terms of both path quality and convergence speed is ultimately selected.

Table 1 Key parameters and values of the LAO algorithm

Parameter	Meaning	Value
m	Number of ants	50
T	Maximum number of iterations	100
α	Importance factor of pheromone	1
β	Importance factor of heuristic function	3
ρ	Pheromone volatilization factor	0.2
L	Proportion of leader ants	0.2
μ_1	Weight of path distance	0.6
μ_2	Weights for path height difference	0.3
μ_3	Weight of obstacle penalty	0.1
μ_4	Weights for reachability	0 or 1
μ_5	Weight of height factor	0.2
μ_6	Weights for distance factor	0.5
μ_7	Weights for smoothness factor	0.3

4.2. Orchard 3D map construction

Obstacles in the orchard mainly include trees, shrubs, fences, small buildings (e.g., tool shed), roads, etc. The height values reflect the relative heights of these obstacles and have a certain distribution pattern in different areas. The central area and some of the edges are set up as a concentration of fruit trees with height values in the range of 5–10 m. Scattered high values indicate buildings, with height values in the 11–13 m range. Lower values indicate fences or shrubs with height values between 1.2–5 m. Certain blank areas, with height values of 0, simulate open spaces or roads and indicate passable areas. In order for the experiment to be presented in a better way, the above data values are enlarged by a factor of 160, resulting in the 3D map shown in Figure 2.

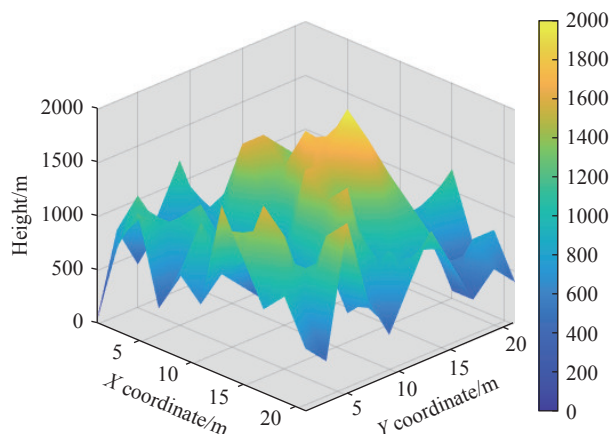


Figure 2. 3D map of the orchard.

4.3. Path quality

The evaluation of path quality consists of two main components: path length and obstacle avoidance. The path length is an evaluation of the total length of the final path, which is a weighted sum of the horizontal and vertical distances. A shorter path means that the ant has chosen a more optimal path. The mean path length of the proposed LAO algorithm is compared with the conventional GA, PSO and ACO algorithms, as shown in Table 2. The mean path lengths of the four algorithms GA, PAO, ACO and LAO are 2487.4956m, 5716.9719m, 4818.4120m and 53.7401m, respectively. It can be seen that the mean path length of the LAO algorithm is significantly lower than the other three algorithms. It shows that the proposed LAO algorithm has good optimality in 3D path planning.

Table 2 Mean performance comparison of GA, PSO, ACO, and LAO algorithms (based on 100 trials)

Algorithm	Mean path length (m)	Mean fitness value	Mean iterations	Mean time (s)
GA	2487.4956	160.4029	48.6	0.0077
PSO	5716.9719	130.6052	88.1	0.2944
ACO	4818.4120	121.3061	84.0	0.2838
LAO	53.7401	44.8481	62.4	0.1021

In addition to the length of the path, it is also necessary to ensure that the path does not cross obstacles. A dynamic obstacle threshold is set for the experiment. In terms of obstacle avoidance, it can be evaluated by detecting whether the path avoids obstacles such as fruit trees, bushes, and buildings. The processing effect of obstacle avoidance directly affects the effectiveness and feasibility of the algorithm. The path planning of the four algorithms LAO, GA, PSO and ACO on 3D cubic space is shown in Figure 3. The two green circles in the figure indicate the start and end points of the path, respectively. A 3D rotation observation of Figure 3 finds that the LAO and ACO algorithms can effectively avoid 3D obstacles. The GA and PSO algorithms, however, often collide with obstacles. Figure 4 shows a plan view presentation of the 3D optimal paths planned by the four obstacle avoidance algorithms. It can be seen that the LAO and ACO algorithms are continuous, which means that the planned 3D paths do not collide with obstacles. While the paths planned by the GA and PSO algorithms have a lot of disconnections, indicating that the paths collide with obstacles, so this path is invalid. Figure 5 shows a 3D perspective view of the optimal paths being planned by these four algorithms. It can be clearly seen that the paths planned by the GA and PSO algorithms pass through the interior of the obstacles and the planned paths have a lot of ups and downs. While the paths planned by LAO and ACO algorithms have better smoothness in the 2D plane and are overall smoother, as shown in Figure 6. In addition, the proposed LAO algorithm is designed to take into account the effect of the height on the UAV flight. From Table 2, it can be learned that the mean path length of the ACO algorithm is much larger than that of the LAO algorithm, but the difference between the paths of the LAO algorithm and the ACO algorithm

in the 2D plane is not significant. Therefore, the ACO algorithm has more ups and downs in the height, which puts a burden on the UAV in terms of flight distance. The LAO algorithm, on the other hand, has less ups and downs in the height, and the algorithm has good smoothness.

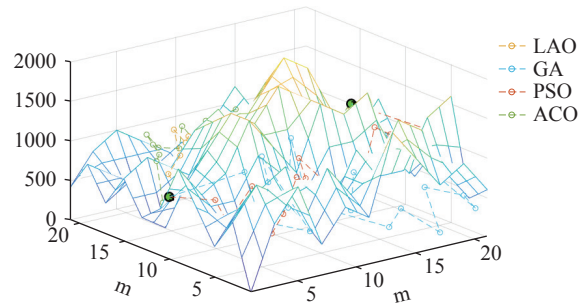


Figure 3. 3D path planning cubic space diagram.

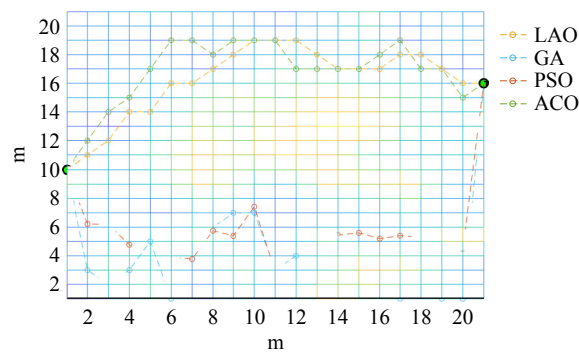


Figure 4. Optimal path obstacle avoidance floor plan.

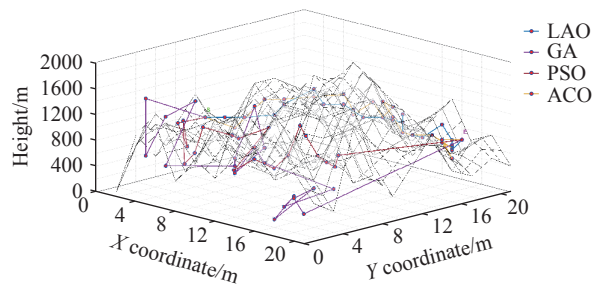


Figure 5. 3D path planning perspective space diagram.

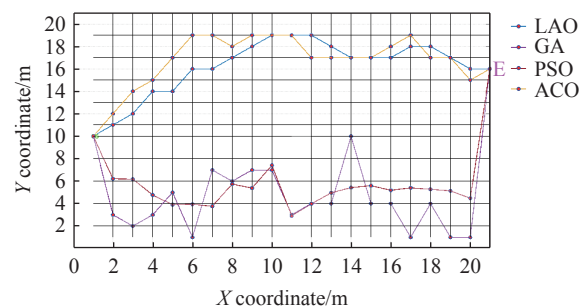


Figure 6. Optimized path floor plan.

4.4. Speed of convergence of the algorithm

Convergence is defined as whether the algorithm is able to find a better solution in a shorter number of iterations or stabilizes after a certain number of iterations. The convergence of the algorithm can be measured by observing the trend of the fitness value. The trend of the best individual fitness of the four algorithms LAO, GA, PSO and ACO is shown in [Figure 7](#), which shows the fluctuation of the fitness of these four algorithms. Among them, the LAO algorithm shows fast convergence and the fitness value stabilizes in a shorter number of iterations. Faster

convergence means that the algorithms can quickly find a better path without wasting too much computational resources. The PSO and ACO algorithms converge slowly and require more iterations to find the optimal solution. And the PSO algorithm has more changes in the fitness value before finding the optimal solution, which is very unstable. The convergence speed of the GA is the fastest, but the optimal fitness value after convergence is the largest, and the quality of the solution is poor. As shown in Table 2, the mean fitness values of the four algorithms GA, PSO, ACO and LAO are 160.4029, 130.6052, 121.3061 and 44.8481, respectively. The average number of iterations of the four algorithms GA, PSO, ACO and LAO are 48.6, 88.1, 84.0 and 62.4, respectively. It can be observed that the LAO algorithm achieves a significantly lower mean fitness value compared to the other three algorithms, along with a smaller average number of iterations, demonstrating good convergence performance.

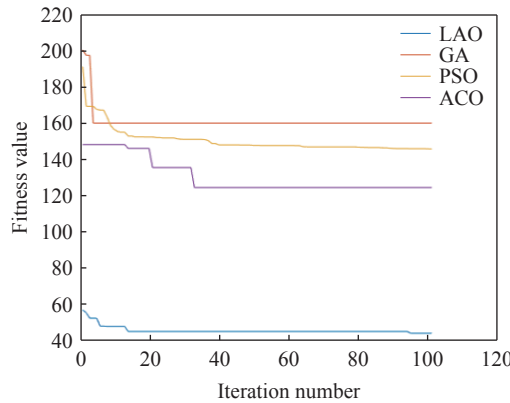


Figure 7. Trends in optimal individual fitness.

4.5. Computational efficiency

The computational efficiency of an algorithm is one of the most important measures of an algorithm's performance, reflecting the resource consumption required to execute the algorithm for a given input size. In path planning, computational efficiency directly affects the practicality of the algorithm. The time required for the algorithm to complete the task in actual operation is a direct way to experimentally evaluate the computational efficiency. As shown in Table 2, the average computation times of the four algorithms GA, PSO, ACO and LAO are 0.0077 s, 0.2944 s, 0.2838 s and 0.1021 s, respectively. It can be observed that the LAO algorithm has a shorter computation time, outperforming the PSO and ACO algorithms, and exhibits good response speed in 3D path planning. However, compared to the GA, there is still room for improvement.

4.6. Statistical Significance Analysis

To further verify the effectiveness of the LAO algorithm, a statistical significance analysis was performed on four evaluation indexes, shortest path length, optimal fitness value, convergence generations, and computation time, compared with the three classical algorithms, including GA, PSO, and ACO, as shown in Table 3. Each algorithm is run independently 100 times under the same experimental conditions, and the resulting experimental data are compared using a two-tailed t-test ($p < 0.05$) to determine whether the differences between the different algorithms are statistically significant.

Table 3 Comparison of p-values for LAO and other algorithms

Comparison		Shortest path length (m)	Optimal fitness value	Convergence generation	Computation time (s)
LAO vs GA	p-value	8.5457×10^{-28}	1.5759×10^{-41}	0.0856	5.5648×10^{-23}
	Significance	Yes	Yes	No	Yes
LAO vs PSO	p-value	1.5992×10^{-19}	6.5787×10^{-18}	0.0008	1.7395×10^{-10}
	Significance	Yes	Yes	Yes	Yes
LAO vs ACO	p-value	1.4864×10^{-16}	3.4608×10^{-17}	0.0038	4.6342×10^{-11}
	Significance	Yes	Yes	Yes	Yes

Comparing LAO algorithm with GA, PSO, and ACO algorithms, the p-value of shortest path length, optimal fitness value, and computation time are all less than 0.01, indicating that these performance differences are statistically significant. The LAO algorithm has a clear advantage in terms of path optimization capability and efficiency. With respect to the convergence generations, the average number of iterations required by the LAO algorithm is significantly less than that of the PSO and ACO algorithms ($p < 0.01$), while the difference is insignificant when compared to the GA ($p > 0.05$). It is shown that the LAO algorithm converges faster and has good

responsiveness in 3D path planning.

In summary, the statistical significance analysis shows that the LAO algorithm outperforms the traditional GA, PSO, and ACO algorithms in terms of path distance, fitness value, and computational speed. It shows superior performance in 3D obstacle avoidance path planning and also has certain advantages in convergence.

5. Conclusions

In this paper, the LAO algorithm is proposed by combining the ACO algorithm and the bellwether theory. The leader has an important leadership role in the flock, which can be used to improve the search efficiency and path quality of the ACO algorithm. In addition, a 3D path planning model is constructed by considering the influence of complex orchard environment on UAV obstacle avoidance. According to the orchard has the characteristics of large terrain ups and downs and uneven distribution of multiple obstacles, the adaptation function, heuristic information and pheromone updating strategy in the ACO algorithm are improved. It makes the planned 3D path more suitable for precise operation in orchard. The experimental simulation results show that the LAO algorithm has higher path planning efficiency, better optimal solution, and lower computation time than the traditional ACO, GA and PSO algorithms. And it can also better avoid obstacles, and adapt to the variability of the orchard environment.

The proposed 3D obstacle avoidance path planning method based on the improved ACO algorithm provides an effective solution for the precise operation of agricultural UAVs and has a broad application prospect. However, the algorithm still has some limitations. Firstly, the LAO algorithm may suffer from sub-optimal path selection with significant dynamic changes in the environment. secondly, the lack of comparison with the recent state-of-the-art methods in the field of 3D path planning limits the competitiveness and broader applicability of the LAO algorithm. Future research can further integrate with 3D visual perception and robotics to improve the applicability and real-time performance of the algorithm in dynamic environments.

Author Contributions: Yi Shao and Hua Yang were involved in the conception and design, or analysis and interpretation of the data; Yi Shao, Hua Yang and Fuzhong Li were involved in the drafting of the paper, revising it critically for intellectual content; and Yi Shao, Hua Yang, Ruibo Gao and Fuzhong Li were involved in the final approval of the version to be published; and that all authors agree to be accountable for all aspects of the work.

Funding: This study was funded by the Key Research and Development Project of Shanxi Province (grant number 20220214060102), the Shanxi Province Basic Research Program Project (grant number 20210302123408), the Open Project Foundation of Intelligent Information Processing Key Laboratory of Shanxi Province (grant number CICIP2023002), and the Science and Technology Innovation Fund of Shanxi Agricultural University (grant number 2023BQ41).

Data Availability Statement: The data that support the findings of this study are available on request from the corresponding author.

Conflicts of Interest: The authors declare no conflict of interest.

References

1. Guebsi, R.; Mami, S.; Chokmani, K. Drones in precision agriculture: A comprehensive review of applications, technologies, and challenges. *Drones* **2024**, *8*, 686. doi: [10.3390/drones8110686](https://doi.org/10.3390/drones8110686)
2. Radoglou-Grammatikis, P.; Sarigiannidis, P.; Lagkas, T.; *et al.* A compilation of UAV applications for precision agriculture. *Comput. Netw.* **2020**, *172*: 107148. doi: [10.1016/j.comnet.2020.107148](https://doi.org/10.1016/j.comnet.2020.107148)
3. Wang, G.B.; Han, Y.X.; Li, X.; *et al.* Field evaluation of spray drift and environmental impact using an agricultural unmanned aerial vehicle (UAV) sprayer. *Sci. Total Environ.* **2020**, *737*: 139793. doi: [10.1016/j.scitotenv.2020.139793](https://doi.org/10.1016/j.scitotenv.2020.139793)
4. Wang, P.A.; Hanif, A.S.; Yu, S.H.; *et al.* Development of an autonomous drone spraying control system based on the coefficient of variation of spray distribution. *Comput. Electron. Agric.* **2024**, *227*: 109529. doi: [10.1016/j.compag.2024.109529](https://doi.org/10.1016/j.compag.2024.109529)
5. Ahmed, S.; Qiu, B.J.; Ahmad, F.; *et al.* A state-of-the-art analysis of obstacle avoidance methods from the perspective of an agricultural sprayer UAV's operation scenario. *Agronomy* **2021**, *11*: 1069. doi: [10.3390/agronomy11061069](https://doi.org/10.3390/agronomy11061069)
6. Bai, Y.H.; Zhang, B.H.; Xu, N.M.; *et al.* Vision-based navigation and guidance for agricultural autonomous vehicles and robots: A review. *Comput. Electron. Agric.* **2023**, *205*: 107584. doi: [10.1016/j.compag.2022.107584](https://doi.org/10.1016/j.compag.2022.107584)
7. Wang, D.S.; Li, W.; Liu, X.G.; *et al.* UAV environmental perception and autonomous obstacle avoidance: A deep learning and depth camera combined solution. *Comput. Electron. Agric.* **2020**, *175*: 105523. doi: [10.1016/j.compag.2020.105523](https://doi.org/10.1016/j.compag.2020.105523)
8. Uğur, A. Path planning on a cuboid using genetic algorithms. *Inf. Sci.* **2008**, *178*: 3275-3287. doi: [10.1016/j.ins.2008.04.005](https://doi.org/10.1016/j.ins.2008.04.005)
9. Phung, M.D.; Ha, Q.P. Safety-enhanced UAV path planning with spherical vector-based particle swarm optimization. *Appl. Soft Comput.* **2021**, *107*: 107376. doi: [10.1016/j.asoc.2021.107376](https://doi.org/10.1016/j.asoc.2021.107376)
10. Zhang, Z.; Wu, J.; Dai, J.Y.; *et al.* Optimal path planning with modified A-Star algorithm for stealth unmanned aerial vehicles in 3D network radar environment. *Proc. Inst. Mech. Eng., Part G: J. Aerospace Eng.* **2022**, *236*: 72-81. doi: [10.1177/09544100211007381](https://doi.org/10.1177/09544100211007381)

11. Hao, K.; Zhao, J.L.; Li, Z.S.; *et al.* Dynamic path planning of a three-dimensional underwater AUV based on an adaptive genetic algorithm. *Ocean Eng.*, **2022**, *263*: 112421. doi: [10.1016/j.oceaneng.2022.112421](https://doi.org/10.1016/j.oceaneng.2022.112421)
12. Mazaheri, H.; Goli, S.; Nourollah, A. A survey of 3D space path-planning methods and algorithms. *ACM Comput. Surv.*, **2025**, *57*: 1. doi: [10.1145/3673896](https://doi.org/10.1145/3673896)
13. Sun, B.; Niu, N.N. Multi-AUVs cooperative path planning in 3D underwater terrain and vortex environments based on improved multi-objective particle swarm optimization algorithm. *Ocean Eng.*, **2024**, *311*: 118944. doi: [10.1016/j.oceaneng.2024.118944](https://doi.org/10.1016/j.oceaneng.2024.118944)
14. Cui, J.G.; Wu, L.; Huang, X.D.; *et al.* Multi-strategy adaptable ant colony optimization algorithm and its application in robot path planning. *Knowl.-Based Syst.*, **2024**, *288*: 111459. doi: [10.1016/j.knsys.2024.111459](https://doi.org/10.1016/j.knsys.2024.111459)
15. Wu, L.; Huang, X.D.; Cui, J.G.; *et al.* Modified adaptive ant colony optimization algorithm and its application for solving path planning of mobile robot. *Expert Syst. Appl.*, **2023**, *215*: 119410. doi: [10.1016/j.eswa.2022.119410](https://doi.org/10.1016/j.eswa.2022.119410)
16. Hu, G.; Huang, F.Y.; Shu, B.; *et al.* MAHACO: Multi-algorithm hybrid ant colony optimizer for 3D path planning of a group of UAVs. *Inf. Sci.*, **2025**, *694*: 121714. doi: [10.1016/j.ins.2024.121714](https://doi.org/10.1016/j.ins.2024.121714)
17. Jin, B.H.; Sun, Y.; Wu, W.J.; *et al.* Deep reinforcement learning and ant colony optimization supporting multi-UGV path planning and task assignment in 3D environments. *IET Intell. Trans. Syst.*, **2024**, *18*: 1652–1664. doi: [10.1049/itr2.12535](https://doi.org/10.1049/itr2.12535)
18. Meng, R.H.; Sun, A.W.; Wu, Z. J.; *et al.* 3D smooth path planning of AUV based on improved ant colony optimization considering heading switching pressure. *Sci. Rep.*, **2023**, *13*: 12348. doi: [10.1038/s41598-023-39346-5](https://doi.org/10.1038/s41598-023-39346-5)
19. Zhang, C.; Hu, C.X.; Feng, J.R.; *et al.* A self-heuristic ant-based method for path planning of unmanned aerial vehicle in complex 3-D space with dense U-type obstacles. *IEEE Access*, **2019**, *7*: 150775–150791. doi: [10.1109/ACCESS.2019.2946448](https://doi.org/10.1109/ACCESS.2019.2946448)
20. Liu, C.; Wu, L.; Li, G.X.; *et al.* AI-based 3D pipe automation layout with enhanced ant colony optimization algorithm. *Autom. Constr.*, **2024**, *167*: 105689. doi: [10.1016/j.autcon.2024.105689](https://doi.org/10.1016/j.autcon.2024.105689)
21. Sangeetha, V.; Krishankumar, R.; Ravichandran, K.S.; *et al.* Energy-efficient green ant colony optimization for path planning in dynamic 3D environments. *Soft Comput.*, **2021**, *25*: 4749–4769. doi: [10.1007/s00500-020-05483-6](https://doi.org/10.1007/s00500-020-05483-6)
22. Zhang, C.; Wang, H.; Fu, L.H.; *et al.* Three-dimensional continuous picking path planning based on ant colony optimization algorithm. *PLoS One*, **2023**, *18*: e0282334. doi: [10.1371/journal.pone.0282334](https://doi.org/10.1371/journal.pone.0282334)
23. Wang, L.F.; Kan, J. M.; Guo, J.; *et al.* 3D path planning for the ground robot with improved ant colony optimization. *Sensors*, **2019**, *19*: 815. doi: [10.3390/s19040815](https://doi.org/10.3390/s19040815)
24. Duan, H.B.; Yu, Y.X.; Zhang, X.Y.; *et al.* Three-dimension path planning forUCAV using hybrid meta-heuristic ACO-DE algorithm. *Simul. Modell. Pract. Theory*, **2010**, *18*: 1104–1115. doi: [10.1016/j.simpat.2009.10.006](https://doi.org/10.1016/j.simpat.2009.10.006)
25. Guo, N.; Qian, B.; Na, J.; *et al.* A three-dimensional ant colony optimization algorithm for multi-compartment vehicle routing problem considering carbon emissions. *Appl. Soft Comput.*, **2022**, *127*: 109326. doi: [10.1016/j.asoc.2022.109326](https://doi.org/10.1016/j.asoc.2022.109326)
26. Chen, Y.; Wu, J.F.; He, C.S.; *et al.* Intelligent warehouse robot path planning based on improved ant colony algorithm. *IEEE Access*, **2023**, *11*: 12360–12367. doi: [10.1109/ACCESS.2023.3241960](https://doi.org/10.1109/ACCESS.2023.3241960)
27. Pu, X.C.; Xiong, C.W.; Ji, L. H.; *et al.* 3D path planning for a robot based on improved ant colony algorithm. *Evol. Intel.*, **2024**, *17*: 55–65. doi: [10.1007/s12065-020-00397-6](https://doi.org/10.1007/s12065-020-00397-6)
28. Zhang, C.; Zhang, D.; Zhang, M.Y.; *et al.* A three-dimensional ant colony algorithm for multi-objective ice routing of a ship in the Arctic area. *Ocean Eng.*, **2022**, *266*: 113241. doi: [10.1016/j.oceaneng.2022.113241](https://doi.org/10.1016/j.oceaneng.2022.113241)
29. Li, X.J.; Yu, D.M. Study on an optimal path planning for a robot based on an improved ANT colony algorithm. *Control Comput. Sci.*, **2019**, *53*: 236–243. doi: [10.3103/S0146411619030064](https://doi.org/10.3103/S0146411619030064)
30. Zhou, H.; Jiang, Z.Q.; Xue, Y.T.; *et al.* Research on path planning in 3D complex environments based on improved ant colony algorithm. *Symmetry* **2022**, *14*: 1917. doi: [10.3390/sym14091917](https://doi.org/10.3390/sym14091917)
31. Han, Z.H.; Liu, S.G.; Yu, F.; *et al.* A 3D measuring path planning strategy for intelligent CMMs based on an improved ant colony algorithm. *Int. J. Adv. Manuf. Technol.* **2017**, *93*: 1487–1497. doi: [10.1007/s00170-017-0503-y](https://doi.org/10.1007/s00170-017-0503-y)
32. Song, J.F.; Pu, Y.Y.; Xu, X.Y. Adaptive ant colony optimization with sub-population and fuzzy logic for 3D laser scanning path planning. *Sensors* **2024**, *24*: 1098. doi: [10.3390/s24041098](https://doi.org/10.3390/s24041098)
33. Yan, B.; Quan, J.L.; Yan, W.H. Three-dimensional obstacle avoidance harvesting path planning method for apple-harvesting robot based on improved ant colony algorithm. *Agriculture* **2024**, *14*: 1336. doi: [10.3390/agriculture14081336](https://doi.org/10.3390/agriculture14081336)
34. Yu, K.L. An obstacle avoidance method for agricultural plant protection UAV based on the fusion of ultrasonic and monocular vision. In *Proceedings of 2021 International Conference on Medical Imaging and Computer-Aided Diagnosis (MICAD 2021) Medical Imaging and Computer-Aided Diagnosis*; Su, R.D.; Zhang, Y.D.; Liu, H., Eds.; Springer: Singapore, 2022; pp. 426–435. doi: [10.1007/978-981-16-3880-0_45](https://doi.org/10.1007/978-981-16-3880-0_45)
35. Tu, G.T.; Juang, J.G. UAV path planning and obstacle avoidance based on reinforcement learning in 3D environments. *Actuators* **2023**, *12*: 57. doi: [10.3390/act12020057](https://doi.org/10.3390/act12020057)
36. Zhang, G.Q.; Liu, J.D.; Luo, W.; *et al.* A shortest distance priority UAV path planning algorithm for precision agriculture. *Sensors* **2024**, *24*: 7514. doi: [10.3390/s24237514](https://doi.org/10.3390/s24237514)
37. Liu, Z.L.; Wen, S.; Huang, G.F.; *et al.* Agricultural UAV obstacle avoidance system based on a depth image inverse projection algorithm and B-spline curve trajectory optimization algorithm. *Inf. Technol. Control* **2024**, *53*: 736–757. doi: [10.5755/j01.itc.53.3.36021](https://doi.org/10.5755/j01.itc.53.3.36021)
38. Dorigo, M. Optimization, Learning and Natural Algorithms. Ph.D. Thesis, Politecnico di Milano, Milan, 1992.
39. Dorigo, M.; Gambardella, L.M. Ant colonies for the travelling salesman problem. *Biosystems* **1997**, *43*: 73–81. doi: [10.1016/S0303-2647\(97\)01708-5](https://doi.org/10.1016/S0303-2647(97)01708-5)
40. Dorigo, M.; Stützle, T. The ant colony optimization metaheuristic: Algorithms, applications, and advances. In *Handbook of Metaheuristics*; Glover, F.; Kochenberger, G.A., Eds.; Springer: Boston, 2003; pp. 250–285. doi: [10.1007/0-306-48056-5_9](https://doi.org/10.1007/0-306-48056-5_9)

Citation: Shao, Y.; Yang, H.; Gao, R.; *et al.* Three-Dimensional Obstacle Avoidance Path Planning for Agricultural UAV Based on Improved Ant Colony Algorithm. *International Journal of Network Dynamics and Intelligence*. 2025, 4(4), 100028. doi: [10.53941/ijndi.2025.100028](https://doi.org/10.53941/ijndi.2025.100028)

Publisher’s Note: Scilight stays neutral with regard to jurisdictional claims in published maps and institutional affiliations.